Available online at www.sciencedirect.com

SciVerse ScienceDirect

Ceramics International 39 (2013) 6183–6188

CERAMICS INTERNATIONAL

www.elsevier.com/locate/ceramint

# KrF excimer laser irradiated nanoporous $TiO_2$ layers for dye-sensitized solar cells: Influence of laser power density

Ming-Yi Pu[a], Jian-Zhang Chen[a,*], I-Chun Cheng[b]

[a]Graduate Institute of Applied Mechanics, National Taiwan University, Taipei City 10617, Taiwan
[b]Graduate Institute of Photonics and Optoelectronics & Department of Electrical Engineering, National Taiwan University, Taipei City 10617, Taiwan

Received 30 October 2012; received in revised form 26 December 2012; accepted 15 January 2013
Available online 21 January 2013

**Abstract**

This paper reports the performance of dye-sensitized solar cells (DSSCs) with nanoporous $TiO_2$ photoanodes irradiated by KrF excimer laser beams of various power densities. The laser induces surface remelting and solidification to create textures on the $TiO_2$ layers. After laser irradiation, $TiO_2$ also undergoes a phase transition from anatase to rutile; the amount of the transformed phase increases with the laser power density. For dye-anchored $TiO_2$ layers, light absorption increases first and then decreases as the laser power density increases. The assembled cell efficiency, strongly correlated with the photocurrent density, also increases first and then decreases as the laser power density rises. This indicates that laser treatment creates surface textures on $TiO_2$ that improve light trapping in the dye-anchored $TiO_2$ photoanodes, thereby increasing the photocurrent level and cell efficiency. For high laser irradiation power density, the ablation of the $TiO_2$ layer becomes significant, leading to a decrease in cell efficiency. The surface remelting and solidification process reduces the density of the surface recombination centers on $TiO_2$, resulting in an increase of open-circuit voltage.


*Keywords:* Excimer laser; Titania; Dye-sensitized solar cells; Texture

## 1. Introduction

Dye-sensitized solar cells (DSSCs) have become a promising technology for photovoltaics since the great breakthrough achieved in 1991 [1]. In DSSCs, photoelectron generation and transport are separated in two distinct materials. The electrons are excited in dyes, and then transported through the nanoporous photoanodes to the external load. The nanoporous photoanode is thus important in both optical and electrical aspects. Light passes through the photoanodes and is absorbed by the dyes. During the passage of light, light trapping/scattering can greatly influence cell performance. Photoanodes are also transport routes for the electrons. The morphology and electrical properties of the photoanodes strongly affect the electron flows. Therefore, the design and fabrication of the photoanodes can significantly influence cell efficiency [2–17].

There have been several papers reporting on the application of laser technology on $TiO_2$ photoanodes for DSSCs. Pan et al. performed spray deposition of $TiO_2$ nanoparticles using a KrF excimer laser [6]. Kim et al. prepared mesoporous $TiO_2$ photo-electrodes from a colloidal solution of nanopowders using a quasi-continuous-wave UV laser ($\lambda=355$ nm) [18]. The laser-induced forward transfer of nanocrystalline $TiO_2$ was also developed using a pulse UV laser ($\lambda=355$ nm) [19]. A 355 nm laser beam was illuminated from the glass side to enhance the adhesion of nanoporous $TiO_2$ and the glass substrate, resulting in enhanced cell performance of DSSCs [20].

In our previous study, we demonstrated that KrF laser treatment on $TiO_2$ photoanodes can improve DSSC efficiency. The influence of the irradiation pulse number has been investigated. In this paper, we report the influence of laser power density on the properties of nanoporous $TiO_2$. Laser treatment induces the phase transformation of $TiO_2$ from anatase to rutile, increasing in severity as the

*Correspondence to: Graduate Institute of Applied Mechanics, National Taiwan University, No.1 Sec. 4 Roosevelt Rd., Taipei City 10617, Taiwan. Tel./fax: +886 2 3366 5694.
*E-mail address:* jchen@ntu.edu.tw (J.-Z. Chen).

0272-8842/$ - see front matter 
http://dx.doi.org/10.1016/j.ceramint.2013.01.037

power density rises. The performance of DSSCs with laser-treated $TiO_2$ photoanodes is also investigated. The improvement in cell performance mainly results from the improvement of the short-circuit current. An optimal power density is also identified.

## 2. Experimental details

Fluorine-doped tin oxide (FTO) coated glass slides (sheet resistance: 8 Ω/□) were used as the substrates for the DSSCs. The $TiO_2$ pastes (E-solar P300, Everlight Chemical Industrial Co.) were first screen-printed onto the FTO glass, and then subsequently calcined at 510 °C for 15 min. This coating procedure was repeated three times for the $TiO_2$ layer thickness to reach 9 μm. After calcination, the nanoporous $TiO_2$ layers were irradiated by a KrF excimer laser. The number of irradiated laser pulses was fixed at 1000. The laser power density was varied as 0, 40, 80, 120, 160, and 200 J/cm$^2$. The laser irradiation repetition rate was 10 Hz.

The laser-irradiated $TiO_2$ coated FTO substrates were then immersed in a mixed solution of acetonitrile (99.9%, J. T. Baker) and tertiary butyl alcohol (99.9%, J. T. Baker) containing $3 \times 10^{-4}$ M of N719 (Solaronix) for 24 h. The dye-absorbed $TiO_2$ photoanodes were rinsed with ethanol and dried at room temperature. A 10-nm Pt was dc-sputtered onto an FTO glass substrate as the counter electrode, which was assembled with the dye-absorbed $TiO_2$ photoanode with spacers. Thereafter, the liquid electrolyte (E-solar EL 100, Everlight Chemical Industrial Co.) was injected into the assembled cells.

An AM1.5 solar simulator (WACOM, WXS-155S-L2) and a Keithley 2000 electrometer were used to measure the IV curves of the cells. The cells were tested with light illuminated through the FTO substrates. The illuminated cell area was 0.22 cm$^2$. The morphology of the laser-irradiated $TiO_2$ was examined by a scanning electron

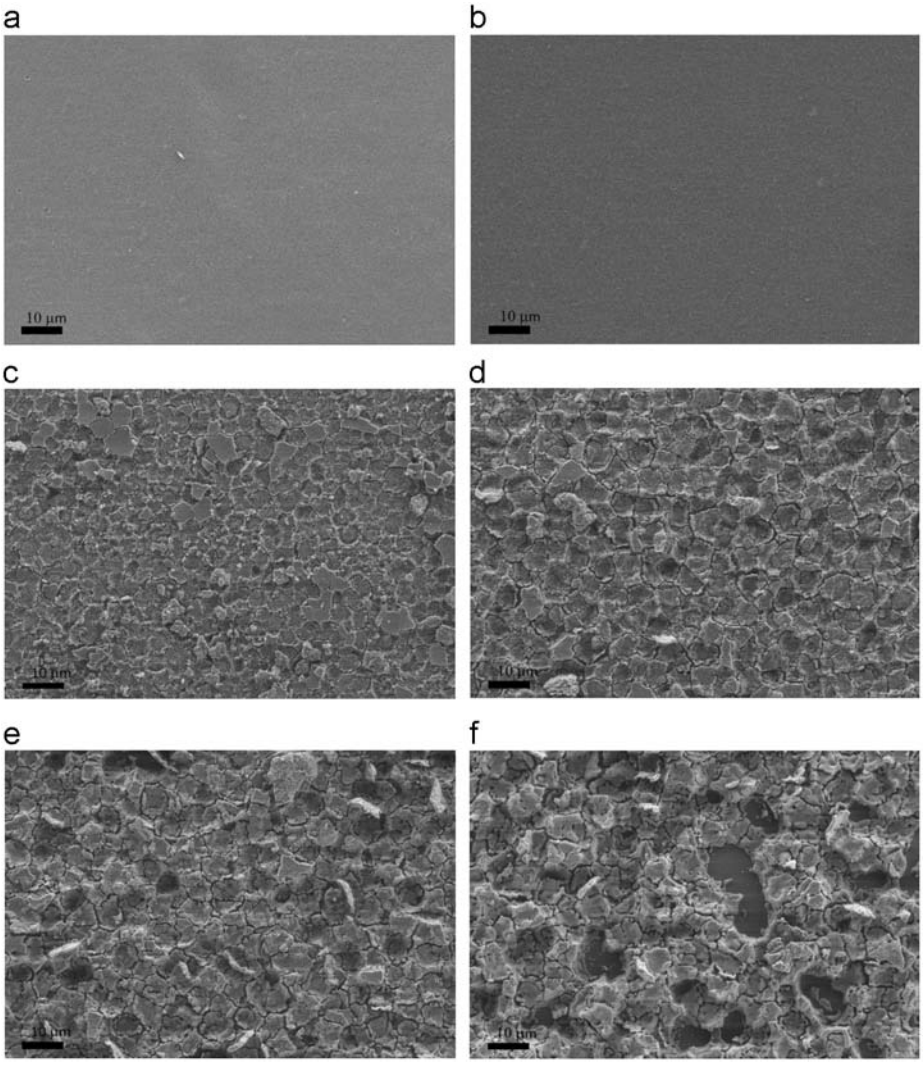


Fig. 1. Low magnifying rate (1000 ×) SEM images of nanoporous $TiO_2$ layers irradiated with various laser power densities: (a) no laser irradiation, (b) 40 mJ/cm$^2$, (c) 80 mJ/cm$^2$, (d) 120 mJ/cm$^2$, (e) 160 mJ/cm$^2$, (f) 200 mJ/cm$^2$.

microscope (SEM, Hitachi S-800). A UV–vis-NIR spectrophotometer (JASCO V-570) with an integration sphere was used to determine the absorption of the dye-anchored $TiO_2$ layers. A field emission scanning electron microscope (FE-SEM, LEO 1530) was used for $TiO_2$ surface morphology inspection. The $TiO_2$ crystal structures were characterized using an X-ray diffractometer (XRD, PANalytical X'Pert PRO) with Cu-$K_\alpha$ radiation ($\lambda = 0.15406$ nm).

## 3. Results and discussion

Fig. 1 shows the 1000 × SEM images of the nanoporous $TiO_2$ layers irradiated with 1000 laser pulses of various laser power densities. The as-calcined nanoporous $TiO_2$ surface is pretty smooth under this magnifying rate, as shown in Fig. 1(a). For the $TiO_2$ irradiated with the laser power density of 40 mJ/cm$^2$, there is some fine structure alternation (shown in Fig. 1(b)) that can be observed more clearly with a 10000 × magnifying rate (Fig. 2(b)). As the power reaches 80 mJ/cm$^2$, the $TiO_2$ surface forms textures and some minor ablation occurs (Fig. 1(c)) Apparent ablation can be clearly identified when the power density is greater than 120 mJ/cm$^2$, increasing in severity as the power density increases (Fig. 1(d)–(f)). A large area of flat surface underneath is revealed as power density reaches 200 mJ/cm$^2$, as shown in Fig. 1(f). Fig. 2 shows SEM images at a higher magnifying rate (10000 ×). The as-calcined nanoporous $TiO_2$ layer is shown in Fig. 2(a). Nanopores can barely be observed. As shown in Fig. 2(b), some cracking can already be observed on the $TiO_2$ surface after laser irradiation with 1000 shots of 40 mJ/cm$^2$ pulse; some of the nanopores have also expanded. As the laser power density reaches 80 mJ/cm$^2$, some remelting and solidification can be identified on the $TiO_2$ surface; the $TiO_2$ surface forms a chip-like structure, as shown in Fig. 2(c). In Fig. 2(d)–(f), it can be clearly observed that the chip size becomes larger as the laser power density increases. Some of the nanopores continue expanding, while some are closed owing to the surface remelting and solidification processes.

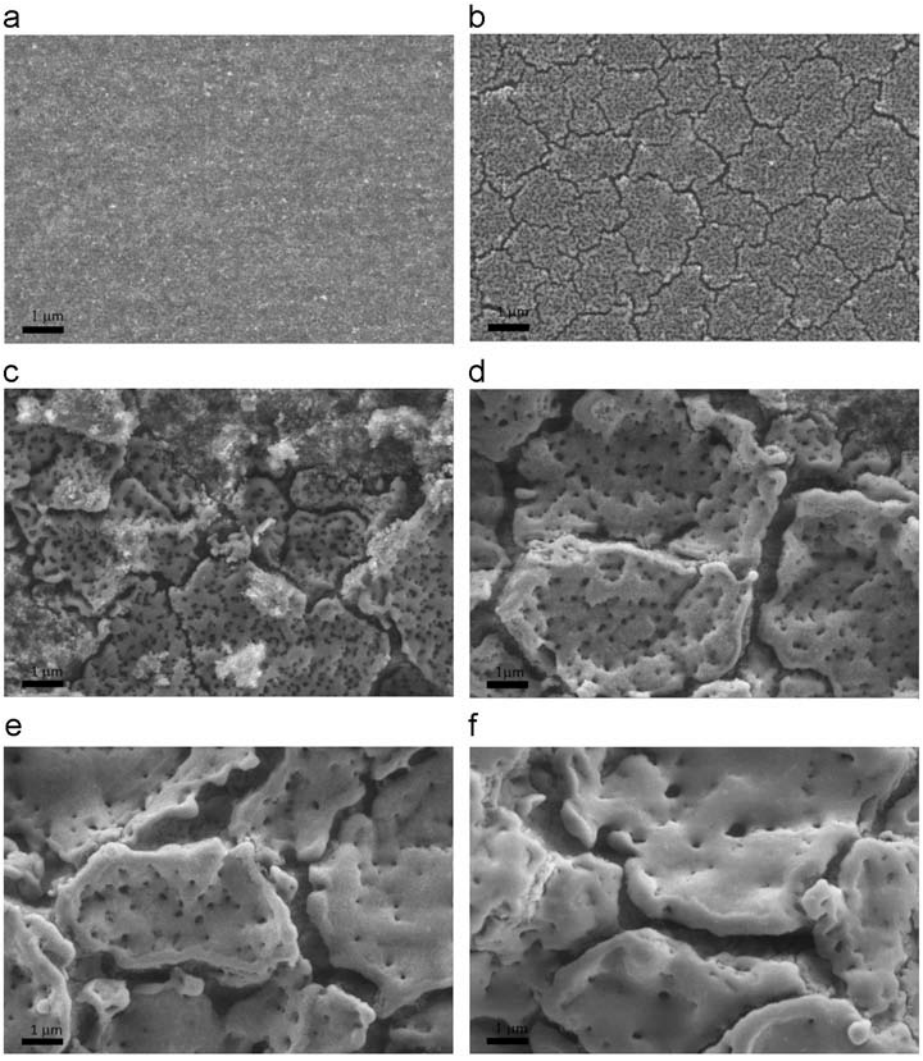


Fig. 2. High magnifying rate (10000 ×) SEM images of nanoporous $TiO_2$ layers irradiated with various laser power densities: (a) no laser irradiation, (b) 40 mJ/cm$^2$, (c) 80 mJ/cm$^2$, (d) 120 mJ/cm$^2$, (e) 160 mJ/cm$^2$ and (f) 200 mJ/cm$^2$.

Fig. 3 shows the XRD patterns for the $TiO_2$ irradiated with various laser power densities. The anatase content $f_A$ is calculated by $f_A=(1+1.26\,I_R/I_A)^{-1}$, where $I_R$ is the (110) rutile phase XRD peak, and $I_A$ is the (101) anatase XRD peak [21,22]. The anatase contents are listed on the right of the XRD patterns. The anatase content significantly decreases as the laser irradiation power density increases. The anatase content is only 46% for $TiO_2$ irradiated with the 200 mJ/cm$^2$ power density, in comparison to 89% for $TiO_2$ without any laser treatments. The laser power density is the dominant factor for the $TiO_2$ phase transformation. Phase transformation of amorphous $TiO_2$ thin films induced by excimer laser irradiation has been studied by Overschelde et al. [23,24]. According to their studies, $TiO_2$ films undergo amorphous-to-anatase and amorphous-to-rutile transformations for low and high fluence KrF excimer laser irradiations, respectively. The anatase phase is more stable in smaller particles, whereas the rutile phase is more stable in larger $TiO_2$ particles. In our case, the used $TiO_2$ pastes contain $TiO_2$ nanoparticles. The calcination process only slightly connects the nanoparticles. After laser irradiation, the anatase $TiO_2$ nanoparticles undergo the remelting and solidification process to merge into a larger piece, in which rutile is the more stable phase. This leads to the anatase-to-rutile phase transformation. The electron transport is slower yet light scattering is more efficient in the rutile phase [25–27]. The increased amount of rutile phase content in the $TiO_2$ layer is favorable optically, but unfavorable electrically.

Fig. 4 shows the absorption spectra for the dye-adsorbed $TiO_2$ layers treated with various laser power densities. The absorption $A$ is defined as $A=1-T-R$, where $T$ and $R$ represent transmission and reflection measured by integration spheres. The absorption increases first and then decreases as the laser power density increases. For the cases of 160 mJ/cm$^2$ and 200 mJ/cm$^2$, absorption is lower than that without any laser treatments, caused by the significant ablation on the $TiO_2$ films. The laser treatment creates surface textures to enhance light trapping and absorption in the nanoporous $TiO_2$ layers. The increased amount of rutile phase after laser irradiation may also enhance light scattering, increasing the light absorption. In the meantime, the surface remelting and solidification process as well as the ablation of the $TiO_2$ layers lead to the decrease of total surface area for dye-anchoring. This will in turn decrease the total absorption.

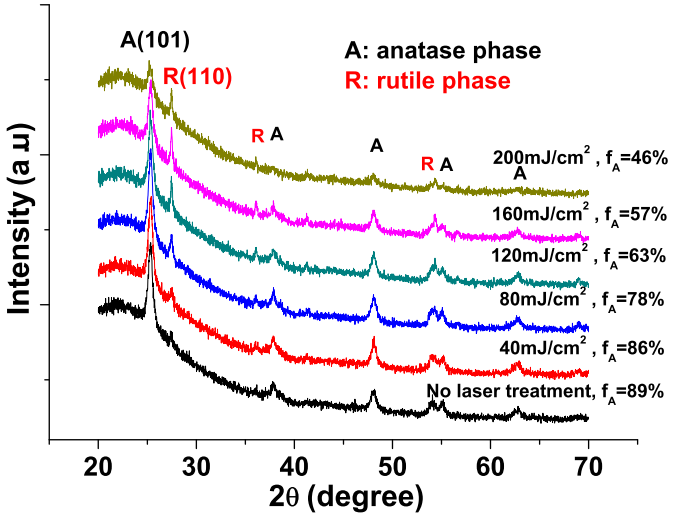


Fig. 3. XRD patterns for nanoporous $TiO_2$ layers irradiated with various laser power densities.

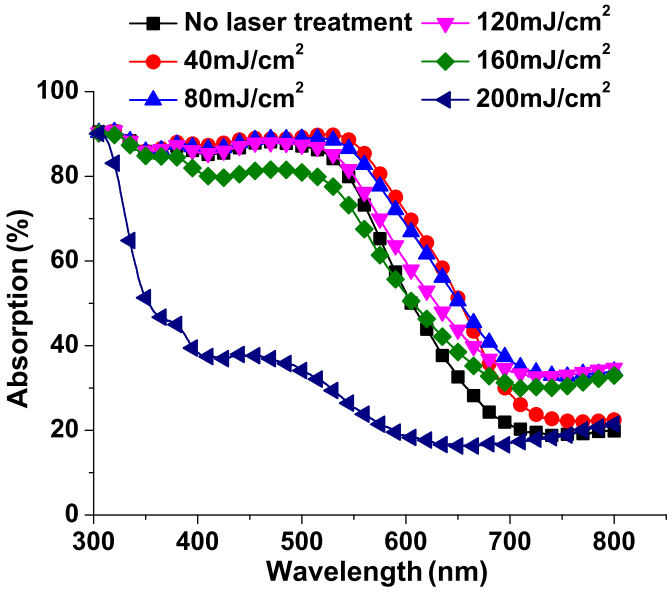


Fig. 4. Absorption spectra of dye-anchored $TiO_2$ layers irradiated with various laser power densities.

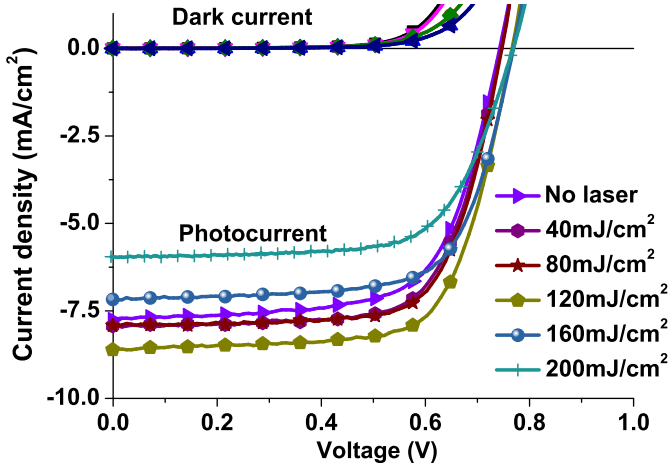


Fig. 5. IV characteristics of DSSCs with $TiO_2$ photoanodes irradiated with various laser power densities.

Fig. 5 shows the IV characteristics of the assembled DSSCs. The cell performance parameters extracted from Fig. 5 are listed in Table 1. Cell efficiency, strongly correlated with the photocurrent level, increases first and then decreases as the power density of the photoanode laser treatment increases. This trend is consistent with the results of the absorption spectra of the dye-anchored $TiO_2$, shown in

Table 1
The DSSC performance parameters extracted from Fig. 5.

| Laser power (mJ/cm$^2$) | Film thickness (μm) | *Voc* (V) | Jsc (mA/cm$^2$) | Fill factor (%) | Efficieny (%) |
|---|---|---|---|---|---|
| **X** | **8.3** | **0.742** | **7.76** | **66.6** | **3.84** |
| **40** | **8.2** | **0.746** | **7.92** | **69.7** | **4.12** |
| **80** | **7.6** | **0.755** | **7.93** | **69.8** | **4.18** |
| **120** | **7** | **0.766** | **8.61** | **69.7** | **4.6** |
| **160** | **5.8** | **0.769** | **7.17** | **69.6** | **3.84** |
| **200** | **4.8** | **0.769** | **5.96** | **68.0** | **3.1** |

Fig. 4. The $TiO_2$ surface textures, created by the laser treatments, enhance light scattering/trapping, improving the photocurrent levels and cell efficiency. The increased amount of rutile $TiO_2$ after laser irradiation may also enhance light scattering, improving the photocurrent levels and cell efficiency. However, when the laser power density is beyond 120 mJ/cm$^2$, the strong ablation of the $TiO_2$ film reduces the total $TiO_2$ volume, leading to the decreasing amount of adsorbed dyes. This reduces the amount of light being absorbed, thereby lowering the photocurrent level and cell efficiency for the DSSCs with photoanodes treated with higher laser power densities. Because the short-circuit current is associated with the photocurrent, the short circuit current increases first and then decreases as the laser irradiation power density increases. The increase of the short-circuit current at the lower laser power density results from the enhancement of light scattering/trapping which improves the light absorption efficiency. On the other hand, the decrease of the short-circuit current at the higher laser power density owes to the reduction of the $TiO_2$ thickness, which causes a decreasing amount of dyes being adsorbed, leading to the reduction of light absorption. The fill factor varies slightly with the laser treatments on the photoanodes. The open-circuit voltage $V_{oc}$ reveals a monotonic increase with the laser power density applied on the $TiO_2$ photoanodes. The surface remelting and solidification process may decrease the density of the surface recombination centers, resulting in the increase in $V_{oc}$ [25–27].

## 4. Conclusions

We investigated the performance of dye-sensitized solar cells (DSSCs) with $TiO_2$ photoanodes irradiated by KrF excimer laser beams of various power densities. Laser treatments create textures on the nanoporous $TiO_2$ surfaces. $TiO_2$ proceeds with an anatase-to-rutile phase transition after laser irradiation. The amount of transformed rutile $TiO_2$ increases with the irradiation laser power density on the $TiO_2$. Cell efficiency, strongly correlated with the photocurrent level and the absorption spectra of the dye-anchored $TiO_2$, increases first and then decreases as the laser power density increases. The open-circuit voltage increases slightly with the applied laser irradiation power density. The enhanced cell efficiency is attributed to improved light trapping, thereby increasing the photocurrent (or short-circuit current) level and cell efficiency. At high laser irradiation power density, the drop in cell efficiency is attributed to the ablation of the $TiO_2$ layer that causes the reduced amount of absorbed dyes. The surface remelting and solidification process also reduces the density of the surface recombination centers, resulting in the increase of the open-circuit voltage.

## Acknowledgments

The authors gratefully acknowledge funding support from the National Science Council of Taiwan under Grant nos. NSC 101-2221-E-002-096 (JZC), NSC 100-2221-E-002-151-MY3, NSC 101-2628-E-002-020-MY3 and NSC 101-3113-E-002-010 (ICC).

## References

[1] B. O'Regan, M. Gratzel, A low-cost, high-efficiency solar cell based on dye-sensitized colloidal $TiO_2$ films, Nature 353 (6346) (1991) 737–740.
[2] Y.F. Gao, M. Nagai, W.S. Seo, K. Koumoto, Template-free self-assembly of a nanoporous $TiO_2$ thin film, Journal of the American Ceramic Society 90 (3) (2007) 831–837.
[3] P.S. Archana, R. Jose, T.M. Jin, C. Vijila, M.M. Yusoff, S. Ramakrishna, Structural and electrical properties of Nb-doped anatase $TiO_2$ nanowires by electrospinning, Journal of the American Ceramic Society 93 (12) (2010) 4096–4102.
[4] R. Jose, V. Thavasi, S. Ramakrishna, Metal oxides for dye-sensitized solar cells, Journal of the American Ceramic Society 92 (2) (2009) 289–301.
[5] D.-W. Liu, I.C. Cheng, J.Z. Chen, H.-W. Chen, K.-C. Ho, C.-C. Chiang, Enhanced optical absorption of dye-sensitized solar cells with microcavity-embedded $TiO_2$ photoanodes, Optics Express 20 (S2) (2012) A168–A176.
[6] H. Pan, S.H. Ko, N. Misra, C.P. Grigoropoulos, Laser annealed composite titanium dioxide electrodes for dye-sensitized solar cells on glass and plastics, Applied Physics Letters 94 (7) (2009) 071117-071117-071113.
[7] C.-P. Hsu, K.-M. Lee, J.T.-W. Huang, C.-Y. Lin, C.-H. Lee, L.-P. Wang, S.-Y. Tsai, K.-C. Ho, EIS analysis on low temperature fabrication of $TiO_2$ porous films for dye-sensitized solar cells, Electrochimica Acta 53 (25) (2008) 7514–7522.
[8] J.Z. Chen, Y.C. Hsu, I.C. Cheng, Enhanced photoelectrochemical performance of photoanode fabricated using polystyrene ball embedded $TiO_2$ pastes, Electrochemical and Solid–State Letters 14 (1) (2011) B6–B8.
[9] Y.C. Hsu, T.C.C. Wu, I.C. Cheng, J.Z. Chen, M.R. Yang, Dye-sensitized solar cell with photoanode made with polystyrene-ball-embedded $TiO_2$ pastes, Japanese Journal of Applied Physics 50 (6) (2011).

[10] M.-Y. Pu, J.Z. Chen, Improved performance of dye-sensitized solar cells with laser-textured nanoporous $TiO_2$ photoanodes, Materials Letters 66 (1) (2012) 162–164.
[11] Y. Xi, W.Z. Wu, H. Fang, C.G. Hu, Integrated ZnO nanotube arrays as efficient dye-sensitized solar cells, Journal of Alloys and Compounds 529 (2012) 163–168.
[12] J. Zhang, W.X. Que, Q.Y. Jia, P. Zhong, Y.L. Liao, X.D. Ye, Y.C. Ding, Novel bilayer structure ZnO based photoanode for enhancing conversion efficiency in dye-sensitized solar cells, Journal of Alloys and Compounds 509 (27) (2011) 7421–7426.
[13] L. Qi, J.D. Sorge, D.P. Birnie, Dye-sensitized solar cells based on $TiO_2$ coatings with dual size-scale porosity, Journal of the American Ceramic Society 92 (9) (2009) 1921–1925.
[14] S.I. Noh, H.J. Ahn, D.H. Riu, Photovoltaic property dependence of dye-sensitized solar cells on sheet resistance of FTO substrate deposited via spray pyrolysis, Ceramics International 38 (5) (2012) 3735–3739.
[15] H.G. Bang, J.K. Chung, R.Y. Jung, S.Y. Park, Effect of acetic acid in $TiO_2$ paste on the performance of dye-sensitized solar cells, Ceramics International 38 (2012) S511–S515.
[16] E.C. Muniz, M.S. Goes, J.J. Silva, J.A. Varela, E. Joanni, R. Parra, P.R. Bueno, Synthesis and characterization of mesoporous $TiO_2$ nanostructured films prepared by a modified sol–gel method for application in dye solar cells, Ceramics International 37 (3) (2011) 1017–1024.
[17] M.N. An'amt, S. Radiman, N.M. Huang, M.A. Yarmo, N.P. Ariyanto, H.N. Lim, M.R. Muhamad, Sol–gel hydrothermal synthesis of bismuth-$TiO_2$ nanocubes for dye-sensitized solar cell, Ceramics International 36 (7) (2010) 2215–2220.
[18] H. Kim, R.C.Y. Auyeung, M. Ollinger, G.P. Kushto, Z.H. Kafafi, A. Piqué, Laser-sintered mesoporous $TiO_2$,; electrodes for dye-sensitized solar cells, Applied Physics A: Materials Science and Processing 83 (1) (2006) 73–76.
[19] H. Kim, G.P. Kushto, C.B. Arnold, Z.H. Kafafi, A. Pique, Laser processing of nanocrystalline TiO[sub 2] films for dye-sensitized solar cells, Applied Physics Letters 85 (3) (2004) 464–466.
[20] J. Kim, J. Kim, M. Lee, Laser welding of nanoparticulate $TiO_2$ and transparent conducting oxide electrodes for highly efficient dye-sensitized solar cell, Nanotechnology 21 (34) (2010).
[21] R.A. Spurr, Quantitative analysis of anatase-rutile mixtures with an X-ray diffractometer, Analytical Chemistry 29 (5) (1957) 760–762.
[22] S.M. Oh, T. Ishigaki, Preparation of pure rutile and anatase $TiO_2$ nanopowders using RF thermal plasma, Thin Solid Films 457 (1) (2004) 186–191.
[23] O. Van Overschelde, G. Guisbiers, M. Wautelet, Nanocrystallization of anatase or rutile $TiO_2$ by laser treatment, Journal of Physical Chemistry C 113 (34) (2009) 15343–15345.
[24] O. Van Overschelde, G. Guisbiers, F. Hamadi, A. Hemberg, R. Snyders, M. Wautelet, Alternative to classic annealing treatments for fractally patterned $TiO_2$ thin films, Journal of Applied Physics 104 (10) (2008).
[25] G. Schlichthorl, S.Y. Huang, J. Sprague, A.J. Frank, Band edge movement and recombination kinetics in dye-sensitized nanocrystalline $TiO_2$ solar cells: a study by intensity modulated photovoltage spectroscopy, Journal of Physical Chemistry B 101 (41) (1997) 8141–8155.
[26] S.Y. Huang, G. Schlichthorl, A.J. Nozik, M. Gratzel, A.J. Frank, Charge recombination in dye-sensitized nanocrystalline $TiO_2$ solar cells, Journal of Physical Chemistry B 101 (14) (1997) 2576–2582.
[27] N.G. Park, J. van de Lagemaat, A.J. Frank, Comparison of dye-sensitized rutile- and anatase-based $TiO_2$ solar cells, Journal of Physical Chemistry B 104 (38) (2000) 8989–8994.